IOP Conference Series: Materials Science and Engineering

Crystallization paths in SiO_2-Al_2O_3-CaO system as a genotype of silicate materials

To cite this article: V I Lutsyk and A E Zelenaya 2013 *IOP Conf. Ser.: Mater. Sci. Eng.* **47** 012047

Crystallization paths in SiO_2-Al_2O_3-CaO system as a genotype of silicate materials

V I Lutsyk[1] and A E Zelenaya[1]

[1]Institute of Physical Materials Science (Siberian Branch of Russian Academy of Sciences), Ulan-Ude, Russian Federation

E-mail: vluts@ipms.bscnet.ru

Abstract. The phases trajectories in the fields of primary crystallization of cristobalite (SiO_2^{cr}), tridymite (SiO_2^{tr}), mullite ($3Al_2O_3 \cdot 2SiO_2$) and in a field of liquid immiscibility are analyzed on a basis of computer model for T-x-y diagram of SiO_2-Al_2O_3-CaO system. The concentration fields with unique set of microconstituents and the fields without individual crystallization schemes and microconstituents are revealed.

1. Introduction

A phase diagram of system SiO_2-Al_2O_3-CaO (S-A-C) has wide applications and can be used in the cement industry to describe the properties of Portland and aluminous cements [1-3], and in studies of refractories and alkali-free glass [4]. To extend the capabilities of research and examine the processes of crystallization for S-A-C system allows its computer model [5-6]. Analysis of concentration fields obtained by the projection of phase regions onto Gibbs triangle allows to establish the boundaries of phase regions (located above the considered fields), the sequence of phase transformations and microstructural elements in crystallized initial melt at the equilibrium condition. Based on this technology, the research identifies fields with coinciding sets of crystallization scheme and microconstituents and the fields with individual characteristics.

2. T-x-y diagram model for SiO_2-Al_2O_3-CaO (S-A-C) system

The experimental data about the structure of S-A-C presented in the literature is usually confined to the surface of the primary crystallization (figure 1a) and triangles of coexistent phases [1-2, 7-9]. The spatial scheme of mono and invariant equilibria permits to restore the full construction of phase diagram. In the first stage a position of invariant planes are reproduced (figure 1b). Then the ruled surfaces of three-phase region borders are formed.

Let's consider the fragment of scheme adjoining to the component SiO_2 (figure 1c). The plane of four-phase regrouping of phases $L_U+SiO_2^{cr} \leftrightarrows R_5+SiO_2^{tr}$ has a degenerated structure U-$R5_U$-$S1_U$($S2_U$) ($S1=SiO_2^{cr}$ and $S2=SiO_2^{tr}$, ^{cr} – cristobalite, ^{tr} - tridymite), because the points $S1_U$ and $S2_U$ coincide together. Two ruled surfaces $S1_{e4}$-e_4-U-$S1_U$ and $R5_{e4}$-e_4-U-$R5_U$ bounding the phase region L+S1+R5 fit to the plane. The plane of ternary eutectic point E_4: $L^{E4} \rightarrow S2^{E4}+R5^{E4}+R12_2^{E4}$ ($S2_{E5}$-$R5_{E5}$-$R12_{E5}$) is arranged below. Three pairs of ruled surfaces ($S2_U$-U-E_5-$S2_{E5}$, $R5_U$-U-E_5-$R5_{E5}$; $S2_{E4}$-E_4-[E_4,E_5]-$S2_{E4,E5}$, $R12_{E4}$-E_4-[E_4,E_5]-$R12_{[E4,E5]}$; $R5_{Q8}$-Q_8-E_5-$R5_{E5}$, $R12_{Q8}$-Q_8-E_5-$R12_{E5}$) are bounded the phase regions L+S2+R5, L+S2+R12, L+R5+R12. The ruled surfaces $S2_{E4}$-E_4-[E_4,E_5]-$S2_{E4,E5}$, $R12_{E4}$-E_4-[E_4,E_5]-$R12_{[E4,E5]}$ are formed from the maximum point [E_4,E_5] on monovariant curve E_4E_5. Three-phase region S2+R5+R12 situates below the simplex $S2_{E5}$-$R5_{E5}$-$R12_{E5}$.

Step-by-step restoring of phase regions boundaries permits to obtaine the complete model of phase diagram (figure 1d).

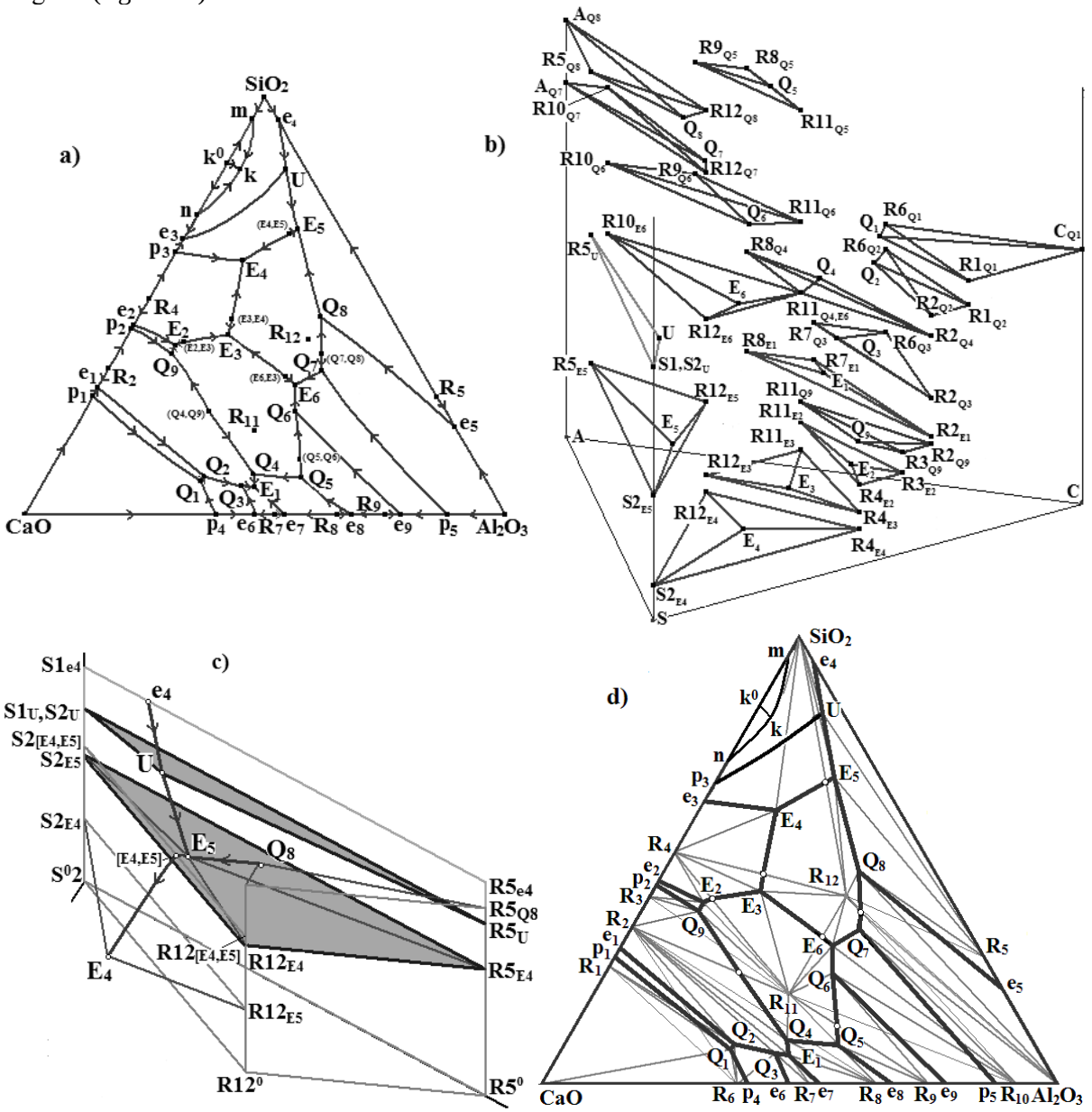

Figure 1. XY projection of primary crystallization surfaces (a); 3D scheme of invariant planes arrangement (b) and three-phase regions of diagram fragment adjoining to the component S (c); XY projection of all phase regions (d) (R_1=C_3S, R_2=C_2S, R_3=C_3S_2, R_4=CS, R_5=A_3S_2, R_6=C_3A, R_7=$C_{12}A_7$, R_8=CA, R_9=CA_2, R_{10}=CA_6, R_{11}=C_2AS, R_{12}=CAS_2).

The projection of phase regions of system S-A-C divides the Gibbs triangle onto 117 two-dimensional, 163 one-dimensional and 45 zero-dimensional concentration fields. It is previously found that the projection of primary crystallization fields CaO, C_3S and C_3A are divided onto 52 concentration fields (19 two-, 21 one- and 12 zero-dimensional), among which 18 fields (12 one- and 6 zero-dimensional) haven't unique set of microconstituents [10].

Let's consider the fragment of phase diagram adjoining to component SiO_2 and carry out the analysis of concentration fields under the surfaces of primary crystallization cristobalite (SiO_2^{cr}), tridymite (SiO_2^{tr}), mullite (A_3S_2) and a cupola of melt immiscibility (i).

3. Structure of phase diagram adjacent to component SiO_2

There are 18 ruled surfaces, 4 horizontal planes at the temperatures of invariant points (E_4, E_5, Q_8, U), 4 vertical triangulation planes under the fields of primary crystallization SiO_2^{cr} (surface Q_{S1} with the contour $mknp_3Ue_4S$), SiO_2^{tr} (Q_{S2} – $e_3E_4[E4,E5]E_5Up_3$), A_3S_2 (Q_{A3S2} – $e_4UE_5Q_8e_5R5$) and the surface of immiscibility melt (i – k^0nkm) (figure 2, table 1). The following designations are used: e and p – binary eutectic and peritectic points, m and n – binary points of monotectic segment, E and Q – ternary eutectic and quasiperitectic points, U – point of the four-phase regrouping with participation of two polymorphous modifications SiO_2^{cr} and SiO_2^{tr}, [E_4,E_5] – maximum point on the monovariant curve E_4E_5.

16 phase regions are located under the considered fields of primary crystallization: L_1+L_2, L+S1, L+S2, L+A_3S_2, S+CAS_2, A+CAS_2, CS+CAS_2, A_3S_2+CAS_2, L_1+L_2+S1, L+S1+S2, L+S2+CS, L+S2+CAS_2, L+A_3S_2+CAS_2, S2+CS+CAS_2, A+A_3S_2+CAS_2, S+A_3S_2+CAS_2 (table 2). The phase region L+S1+S2 is degenerated into line and the corresponding phase reaction proceeds at one temperature.

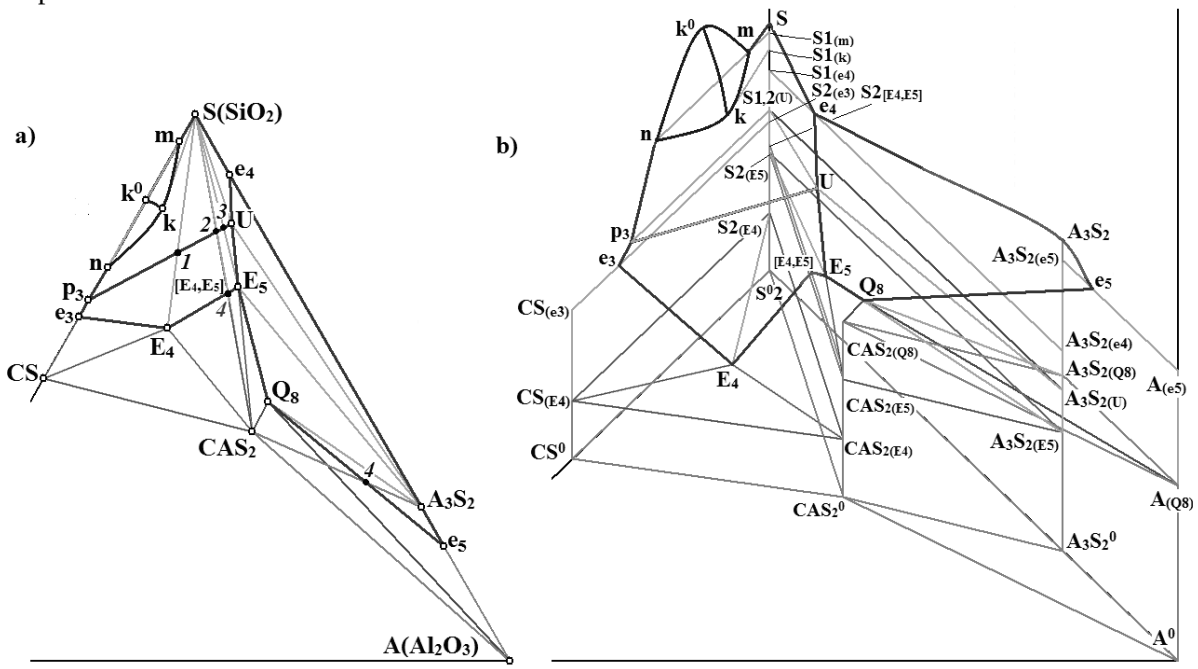

Figure 2. XY projection (a) and 3D model (b) of fragment of system S-A-C phase diagram.

Table 1. Contours of ruled surfaces (Q^r, i^r), horizontal (H) and vertical (V) planes.

Symbol	Contour	Symbol	Contour
$Q^r_{e4\_A3S2}$	$A_3S_{2(e4)}$-e_4-U-$A_3S_{2(U)}$	$Q^r_{E4E5\_R12}$	$CAS_{2(E4)}$-E_4-[E_4,E_5]- $CAS_{2[E4,E5]}$
$Q^r_{E5U\_A3S2}$	$A_3S_{2(U)}$-U-E_5-$A_3S_{2(E5)}$	$Q^r_{E5E4\_R12}$	$CAS_{2(E5)}$-E_5-[E_4,E_5]- $CAS_{2[E4,E5]}$
$Q^r_{Q8E5\_A3S2}$	$A_3S_{2(Q8)}$-Q_8-E_5-$A_3S_{2(E5)}$	i^r	m-k-n
$Q^r_{e5\_A3S2}$	$A_3S_{2(e5)}$-e_5-Q_8-$A_3S_{2(Q8)}$	i^r_m	$S1_{(mn)}$-m-k-$S1_{(k)}$
$Q^r_{e4\_S}$	$S1_{(e4)}$-e_4-U-$S1_{(U)}$	i^r_n	$S1_{(mn)}$-n-k-$S1_{(k)}$
$Q^r_{E5U\_S}$	$S2_{(U)}$-U-E_5-$S2_{(E5)}$	H_{E4}	$S2_{(E4)}$-CS_{E4}-$CAS_{2(E4)}$
$Q^r_{e5\_A}$	$A_{(e5)}$-e_5-Q_8-$A_{(Q8)}$	H_{E5}	$S2_{E5}$-$A_3S_{2(E5)}$-$CAS_{2(E5)}$
$Q^r_{Q8E5\_CAS2}$	$CAS_{2(Q8)}$-Q_8-E_5- $CAS_{2(E5)}$	H_{Q8}	Q_8-$A_3S_{2(Q8)}$-A-$CAS_{2(Q8)}$

$Q^r_{e3\_S}$	$S2_{(e3)}$-e_3-E_4-$S2_{(E4)}$	H_U	U-$A_3S_{2(U)}$-$S1_{(U)}$,$S_{2(U)}$
$Q^r_{p3\_S}$	$S1_{(U)}$-p_3-U	$V_{S\text{-}CAS2}$	$S2_{[E4,E5]}$-$CAS_{2[E4,E5]}$-CAS_2^0-$S2^0$
$Q^r_{E4E5\_S}$	$S2_{(E4)}$-E_4-[E_4,E_5]-$S2_{[E4,E5]}$	$V_{A\text{-}CAS2}$	A_{Q8}-$CAS_{2(Q8)}$-CAS_2^0-$A_3S_2^0$
$Q^r_{E5E4\_S}$	$S2_{(E5)}$-E_5-[E_4,E_5]-$S2_{[E4,E5]}$	$V_{R5\text{-}CAS2}$	$A_3S_{2(Q8)}$-$CAS_{2(Q8)}$-CAS_2^0-$A_3S_2^0$
$Q^r_{e3\_CS}$	E_3-E_4-CS_{E4}-CS_{e3}	$V_{R4\text{-}CAS2}$	$CS_{(E4)}$-$CAS_{2(E4)}$-CAS_2^0-CS^0

Table 2. Phase regions structure.

Symbol	Bounding surfaces	Symbol	Bounding surfaces
L_1+L_2	i, i^r	L+A_3S_2+CAS_2	$Q^r_{Q8E5\_A3S2}$, $Q^r_{Q8E5\_CAS2}$, H_{Q8}, H_{E5}, $V_{A3S2\text{-}CAS2}$
L+S1	Q_{S1}, i^r, $Q^r_{e4\_S}$, $Q^r_{p3\_S}$	S2+CS+CAS_2	$V_{S\text{-}CAS2}$, $V_{CS\text{-}CAS2}$, H_{E4}
L+S2	Q_{S2}, $Q^r_{e3\_S}$, $Q^r_{p3\_S}$, $Q^r_{E5U\_S}$, $Q^r_{E4E5\_S}$, $Q^r_{E5E4\_S}$	A_3S_2+ CAS_2+A	H_{Q8}, $V_{A\text{-}CAS2}$, $V_{A3S2\text{-}CAS2}$
L+A_3S_2	Q_{A3S2}, $Q^r_{e4\_A3S2}$, $Q^r_{E5U\_A3S2}$, $Q^r_{Q8E5\_A3S2}$, $Q^r_{e5\_A3S2}$	S2+A_3S_2+CAS_2	$V_{A3S2\text{-}CAS2}$, $V_{S\text{-}CAS2}$, H_{E5}
L_1+L_2+S1	i^r, i^r_n, i^r_m	S2+CAS_2	$V_{S\text{-}CAS2}$
L+S1+S2	$Q^r_{p3\_S}$	A+CAS_2	$V_{A\text{-}CAS2}$
L+S2+CS	$Q^r_{e3\_CS}$, $Q^r_{e3\_S}$, H_{E4}	A_3S_2+CAS_2	$V_{A3S2\text{-}CAS2}$
L+S2+CAS_2	$Q^r_{E4E5\_S}$, $Q^r_{E5E4\_S}$, $Q^r_{E5E4\_CAS2}$, $Q^r_{E4E5\_CAS2}$, H_{E4}, H_{E5},$V_{S\text{-}CAS2}$	CS+CAS_2	$V_{CS\text{-}CAS2}$

4. Analysis of the concentration fields

At projection the surfaces Q_{S1}, Q_{S2}, Q_{A3S2} and i are divided onto 15 two-, 28 one- and 9 zero-dimensional concentration fields. Thirteen (2 two-, 8 one-and 3 zero-dimensional) fields coincide with neighbouring fields by the set of microconstituents.

The microconstituents of concentration fields corresponding to the regions of immiscibility melt (m-n-k, SiO_2-m-k, SiO_2-k, n-k, m-k, k) coincide with the of field p_3-1-SiO_2-k-n. Meanwhile the fields m-n-k, SiO_2-m-k and m-k duffer from field p_3-1-SiO_2-k-n by intersected surfaces, phase regions and crystallization scheme (table 3). The phase region L+S_1 and phase region of immiscibility melt L+S_1+S_2 are located under the field SiO_2-m-k. At that the phase region L+S_1 is twice crossed for this field. So the field is characterized by two primary crystallization reactions $L^1 \rightarrow S_1^1$ between which the monotectic reaction $L_1^m \rightarrow L_2^m + S_1^m$ takes place. Field m-n-k arranges under the surface of immiscibility melt (i) and intersects the phase regions L_1+L_2 и L_1+L_2+S_1, where the phase reaction $L_1^1 \rightarrow L_2^1$ и $L_1^m \rightarrow L_2^m + S_1^m$ occur.

Since the process of melt immiscibility ends in the phase region L_1+L_2+B_1, then the reaction products L_2^1 and L_2^m doesn't influence on the microconstituents forming. The crystals B_1 are not present in the microconstituents, because they are fully disappeared in the reactions $L^p,B_1 \rightarrow B_2^p$ and $L^U,S_1 \rightarrow S_2^U + A_3S_2^U$ and in the subsequent phase transformations there are only B_2 crystals. The reactions $L^p,S_1 \rightarrow S_2^p$ and $L^U,S_1 \rightarrow S_2^U + A_3S_2^U$ have degenerated form as the result of degeneration of phase regions L+S_1+S_2 in horizontal line and four-phase plane in the triangle U-$A_3S_{2(U)}$-$S1_{(U)}$,$S_{2(U)}$ [11].

The fields SiO_2-k, n-k and k coincide with field p_3-1-SiO_2-k-n by the list of phase reactions and the microconstituents.

Table 3. Crystallization scheme and microconstituents for surface of immiscibility i and the fragment of primary crystallization surface Q_{S1} of high-temperature modification SiO^{cr}_2 (S1) *.

Concentration fields	Intersected surfaces	Intersected phase regions	Crystallization scheme	Microconstituents
p_3-1-SiO_2-k-n	Q_{S1},	L+S_1,	$L^1 \rightarrow S_1^1$,	
	$Q^r_{p3\text{-}S}$,	L+S_1+S_2,	$L^p + S_1^1 \rightarrow S_2^p$,	S_2^p,
	$Q^r_{e3\text{-}S}$,	L+S_2,	$L^{1p} \rightarrow S_2^{1p}$,	S_2^{1p},

	H_{E4}	$L+S_2+CS$, $B_2+CS+CAS_2$	$L^{ep}\rightarrow S_2^{ep(CS)}+CS_4^{ep(B2)}$ $L^{E4}\rightarrow S_2^{E4}+CS_4^{E4}+CAS_2^{E4}$	$S_2^{ep(CS)}$, $CS^{ep(B2)}$ S_2^{E4}, CS^{E4}, CAS_2^{E4}
SiO_2-m-k	Q_{S1}, i^r_m, i^r_n, Q^r_{p3-S}, Q^r_{e3-S}, H_{E4}	$L+S_1$, $L_1+L_2+S_1$, $L+S_1$, $L+S_1+S_2$, $L+S_2$, $L+S_2+CS$, $S_2+R_4+CAS_2$	$L^1\rightarrow S_1^1$, $L_1^m\rightarrow L_2^m+S_1^m$, $L^1\rightarrow S_1^1$ $L^p+S_1^{1,1p}\rightarrow S_2^p$, $L^{1p}\rightarrow S_2^{1p}$, $L^{ep}\rightarrow S_2^{ep(CS)}+CS^{ep(B2)}$ $L^{E4}\rightarrow S_2^{E4}+CS^{E4}+CAS_2^{E4}$	 S_2^p, S_2^{1p}, $S_2^{ep(CS)}$, $CS^{ep(B2)}$ S_2^{E4}, CS^{E4}, CAS_2^{E4}
m-n-k	i, i^r, i^r_n, Q^r_{p3-S}, Q^r_{e3-S}, H_{E4}	L_1+L_2, $L_1+L_2+S_1$, $L+S_1$, $L+S_1+S_2$, $L+S_2$, $L+S_2+CS$, $S_2+CS+CAS_2$	$L_1^1\rightarrow L_2^1$, $L_1^m\rightarrow L_2^m+S_1^m$, $L^1\rightarrow S_1^1$, $L^p+S_1^1\rightarrow S_2^p$, $L^{1p}\rightarrow S_2^{1p}$, $L^{ep}\rightarrow S_2^{ep(CS)}+CS^{ep(B2)}$ $L^{E4}\rightarrow S_2^{E4}+CS^{E4}+CAS_2^{E4}$	 S_2^p, S_2^{1p}, $S_2^{ep(CS)}$, $CS^{ep(B2)}$ S_2^{E4}, CS^{E4}, CAS_2^{E4}
SiO_2-k	Q_{S1}, Q^r_{p3-S}, Q^r_{e3-S}, H_{E4}	$L+S_1$, $L+S_1+S_2$, $L+S_2$, $L+S_2+CS$, $S_2+R_4+CAS_2$	$L^1\rightarrow S_1^1$, $L^p+S_1^1\rightarrow S_2^p$, $L^{1p}\rightarrow S_2^{1p}$, $L^{ep}\rightarrow S_2^{ep(CS)}+CS^{ep(B2)}$ $L^{E4}\rightarrow S_2^{E4}+CS^{E4}+CAS_2^{E4}$	 S_2^p, S_2^{1p}, $S_2^{ep(CS)}$, $CS^{ep(B2)}$ S_2^{E4}, CS^{E4}, CAS_2^{E4}
n-k	Q_{S1}, Q^r_{p3-S}, Q^r_{e3-S}, H_{E4}	$L+S_1$, $L+S_1+S_2$, $L+S_2$, $L+S_2+CS$, $B_2+R_4+CAS_2$	$L^1\rightarrow S_1^1$, $L^p+S_1^1\rightarrow S_2^p$, $L^{1p}\rightarrow S_2^{1p}$, $L^{ep}\rightarrow S_2^{ep(CS)}+CS^{ep(B2)}$ $L^{E4}\rightarrow S_2^{E4}+CS^{E4}+CAS_2^{E4}$	 S_2^p, S_2^{1p}, $S_2^{ep(CS)}$, $CS^{ep(B2)}$ S_2^{E4}, CS^{E4}, CAS_2^{E4}
m-k	Q_{S1}, i^r_m, i^r_n, Q^r_{p3-B}, Q^r_{e3-B}, H_{E4}	$L+S_1$, $L_1+L_2+S_1$, $L+S_1$, $L+S_1+S_2$, $L+S_2$, $L+S_2+CS$, $S_2+R_4+CAS_2$	$L^1\rightarrow S_1^1$, $L_1^m\rightarrow L_2^m+S_1^m$, $L^1{}_2\rightarrow S_1^1$, $L^p+S_1^{1,1p}\rightarrow S_2^p$, $L^{1p}\rightarrow S_2^{1p}$, $L^{ep}\rightarrow S_2^{ep(CS)}+CS^{ep(B2)}$ $L^{E4}\rightarrow S_2^{E4}+CS^{E4}+CAS_2^{E4}$	 S_2^p, S_2^{1p}, $S_2^{ep(CS)}$, $CS^{ep(B2)}$ S_2^{E4}, CS^{E4}, CAS_2^{E4}

* ^{1} – primary crystallization $L^1\rightarrow I^1$; ^{e} – monovariant eutectic reaction $L^e\rightarrow I^e+J^e$; ^{p} – monovariant peritectic reaction $L^p+A^p\rightarrow R^p$; ^{m} – monovariant monotectic reaction $L_1^m\rightarrow L_2^m+R^m$; ^{E} – invariant eutectic crystallization $L^E\rightarrow B^E+C^E+R^E$; ^{Q} – invariant quasiperitectic regrouping of masses $L^Q+A^Q\rightarrow B^Q+R^Q$; ^{1p} – post-peritectic primary crystallization $L^{1p}\rightarrow R^{1p}$; ^{ep} – post-peritectic monovariant crystallization $L^{ep}\rightarrow R^{ep}+J^{ep}$ (J=B, C).

Let's consider the diagram of mass balances for composition given in the field p_3-1-SiO_2-k-n (figure 3). After the reaction of primary crystallization $L^1\rightarrow S_1^1$ in the phase region L+S1 the composition falls into phase region $L+S_1+S_2$ (degenerated into line) where the crystals S_1 is fully disappeared as the result of reactions $L^p,S_1\rightarrow S_2^p$ and $L^U,S_1\rightarrow S_2^U+A_3S_2^U$. Then the composition moves into the phase region $L+S_2$ where the post-peritectical primary crystallization $L^{1p}\rightarrow S_2^{1p}$ takes place with the increasing of phase part S_2. In the phase region $L+S_2+CS$ the part of phase L is decreased and parts of phases S_2 and CS are increased: ($L^{ep}\rightarrow S_2^{ep(CS)}+CS^{ep(B2)}$). The phase L is fully disappeared as the result of reaction $L^{E4}\rightarrow S_2^{E4}+CS^{E4}+CAS_2^{E4}$ on the plane at the temperature of ternary eutectic points E_4. Below the plane the composition gets to the solid-phase region $S_2+CS+CAS_2$.

The concentration fields e_4-U and U coincide with fields SiO_2-U-e_4 и SiO_2-U by the microconstituents, but differ the crystallization scheme. Fields e_4-U and U haven't the reaction of primary crystallization $L^1 \rightarrow B_1^1$. The concentration fields p_3-1 and 2 differ from fields e_3-E_4-1-p_3 and 2-4 by intersected surfaces. The fields E_5-3, A_3S_2-U и A_3S_2-Q_8 are identical with E_5-U-3, U-E_5- A_3S_2 and E_5-Q_8-A_3S_2 by the microconstituents and crystallization scheme correspondently.

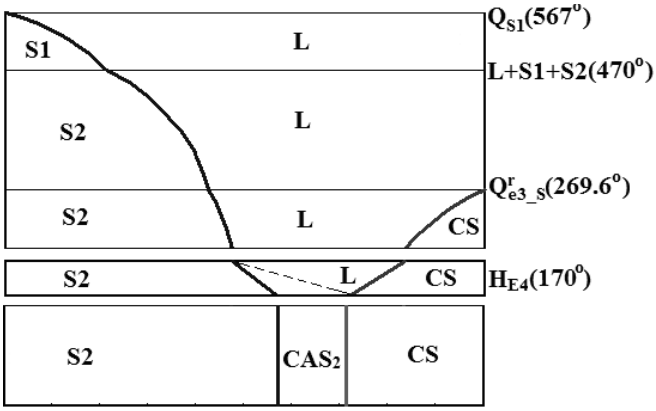

Figure 3. Diagram of material balance for the concentration field p_3-1-SiO_2-k-n.

5. Conclusion

Computer model of PD gives the possibility to analyze the crystallization stages for any composition and to find the concentration fields both with individual set of microstructure elements and the fields at which the crystallization scheme and microconstituents of phases assemblage coincide with those in the adjoining fields. It is used as an important tool to investigate multicomponent system, to correct its constitutional diagram, to design the miscrostructures of heterogeneous material, to decipher the genotype of heterogeneous material [12]. One more reason for the microstructures variety is the competition of crystals with different dispersity, when a field of invariant reaction is divided into the fragments with the tiny eutectical crystals, with more large primary crystals and with the both type of these crystals [13].

References

[1] Taylor H F W 1997 *Cement Chemistry* (London, Thomas Telford)
[2] Lea F 1998 *Lea's Chemistry of Cement and Concrete* (London: P.C. Hewlett)
[3] De Noirfontaine M N, Tusseau-Nenez S et al. 2012 *J. Mater. Sci.* **47** 1471
[4] Pashchenko A A, Aleksenko N V et al. 1977 *Phisical Chemistry of Silicate* ed A A Pashchenko (Kiev: Vyshcha schkola) (In Russian)
[5] Lutsyk V I, Zelenaya A E, Savinov V V 2011 *IOP Conf. Ser.: Mater. Sci. Eng.* **18** http://iopscience.iop.org/1757-899X/18/11/112005/pdf/1757-899X_18_11_112005.pdf
[6] Lutsyk V I, Zelenaya A E, Savinov V V 2012 *Crys. Rep.* **57** 943
[7] Gentile A L, Foster W R 1963 *J. Amer. Cer. Soc.* **46** 74
[8] Levin E M, Robbins C R and McMurdie H F 1964 *Phase Diagrams for Ceramists* (Ohio: American Ceramic Society)
[9] Toropov N A, Bazarkovsky V P, Lapshin V V et al. 1972 *Diagrams of Silicate Systems.* vol 3. *Ternary Silicate Systems* (Leningrad: Nauka) pp 184-190 (In Russian)
[10] Lutsyk V, Zelenaya A 2012 Proc. Int. Conf. Oxide Materials for Electronic Engineering (Lviv, Ukraine) 133
[11] Lukas H L, Henlg E T, Petzow G 1986 *Z. Metallkde.* **77** 360
[12] Lutsyk V I 2012 *Bulletin of Buryat Scientific Centre (SB RAS)* no 1(5), 78 (In Russian)
[13] Lutsyk V I, Nasrulin E R 2012 *Crys. Rep.* **57** 106